Piezoelectric properties of microfabricated $(K,Na)NbO_3$ thin films

Yu Wakasa,[1] Isaku Kanno*,[1] Ryuji Yokokawa,[1] Hidetoshi Kotera,[1] Kenji Shibata,[2] Tomoyoshi Mishima[2]
[1]Micro Engineering, Kyoto University, Yoshida-honmachi, Sakyo-ku, Kyoto 606-8501, Japan
[2]Research and Development Laboratory, Hitachi Cable Ltd., 3550 Kidamari, Tsuchiura, Ibaraki, Japan

Abstract

A novel microfabrication method of lead-free piezoelectric sodium potassium niobate [$(K,Na)NbO_3$, KNN] thin films was proposed, and the piezoelectric characteristics of the KNN microactuators were evaluated. The KNN thin films were directly deposited on microfabricated Si microcantilevers. The transverse piezoelectric coefficient d_{31} of the KNN films was calculated as −53.5 pm/V at 20 V_{pp} from the tip displacement of the microcantilevers. However, the tip displacement showed large electric-field dependence because of the extrinsic piezoelectric effect, and the intrinsic piezoelectric effect of the KNN microcantilevers was smaller than that of KNN on unprocessed thick substrates. In contrast, the extrinsic piezoelectric effect was almost independent of the microfabrication of the KNN films.

Kew Words : KNN, piezoelectric, thin films, microfabrication, MEMS
Corresponding author. Tel.: +81-75-753-3561
E-mail : kanno@mech.kyoto-u.ac.jp

1. INTRODUCTION

Recently, piezoelectric thin films have been widely investigated for their applications in various microelectromechanical systems (MEMS), such as microsensors and microactuators. Lead zirconate titanate [$Pb(Zr,Ti)O_3$, PZT] is one of the most popular materials because of its superior piezoelectric properties, and PZT thin films have been studied as a key material for piezoelectric MEMS [1]. However, PZT-based piezoelectric materials contain toxic lead, making it important to realize lead-free piezoelectric materials with piezoelectric properties comparable to those of PZT, even in the form of thin films. Just after the discovery of piezoelectric sodium potassium niobate [$(K,Na)NbO_3$, KNN]-based ceramics, which have been found to have a high piezoelectric coefficient d_{33} comparable to PZT ceramics [2], the development of lead-free piezoelectric materials has been activated. Considering the practical applications, KNN ceramics are very useful for the piezoelectric devices because of the high Curie temperature of KNN compatible to that of PZT-based piezoelectric materials [3].

To develop the piezoelectric MEMS using lead-free materials, the KNN ceramics have to be prepared in the thin-film form, and successively the KNN thin films should be microfabricated by using photolithograph and wet- or dry-etching process. Recently, the characteristics of the KNN thin films have been reported [4-8]. Shibata *et al*. reported that the KNN thin films deposited by RF magnetron sputtering showed large transverse piezoelectric properties comparable to those of PZT thin films [8]. On the other hand, it is well known that PZT thin films can be easily microfabricated by photolithography and etching processes, such as wet etching with acid solution or dry etching using reactive gases like CF_4 and Cl_2 [9, 10]. However, since KNN is stable to acid or alkali solutions, the etching rate of dry etching using inductively coupled plasma reactive ion etching is considerably low to remove the micrometer-thick KNN films [11]. Because of the difficulty in fabricating the KNN thin films using traditional photolithography and etching processes, Xu *et al*. proposed a new approach for the microfabrication of piezoelectric the KNN thin films. In this approach, the KNN thin films are deposited on a microfabricated Si substrate by using the sol-gel method and the surface is subsequently polished [12]. This method could successfully fabricate microrod structures, but the fabrication process of typical microstructures in MEMS, such as cantilevers and membranes, has not been established yet.

In this study, we propose a novel microfabrication method not only to develop piezoelectric MEMS devices, but also to evaluate the piezoelectric characteristics of the stress-free KNN thin films. We deposited the KNN thin films on Si substrates by RF

magnetron sputtering and fabricated the KNN microcantilevers. We measured their actuator performance on the basis of which we characterized the transverse piezoelectric properties of the microfabricated KNN thin films free from the clamping effect of the thick substrates.

2. Microfabrication of KNN thin films

Figure 1 shows the schematic representation of the fabrication process of the KNN microcantilevers. First, Si microcantilevers were fabricated on silicon-on-insulator (SOI) substrates. The thicknesses of the active Si and buried oxide (BOX) layers of the SOI wafer were 8 and 2 μm, respectively. The active Si layer on the BOX layer was then fabricated into the cantilever-shaped structure by reactive ion etching, and was then released by wet etching of the BOX layer in buffered HF. We fabricated five types of cantilevers, varying in length from 285 to 589 μm, with a constant width of 112 μm.

After fabrication of Si microcantilevers, the piezoelectric KNN films were deposited on them. A Ti adhesion layer (2 nm) and a Pt bottom electrode (200 nm) were deposited by RF magnetron sputtering on the SOI substrates having Si microcantilevers. Then, the 2-μm thick KNN thin films were deposited on the Pt/Ti-coated SOI substrates by RF magnetron sputtering at the substrate temperature of approximately 680 °C in Ar and O_2 mixed gas atmosphere [7, 8]. The chemical composition of the KNN films was approximately Na/(K + Na) = 0.55. Finally, top electrodes (Pt, 150 nm) were deposited and patterned by a lift-off process. The crystal structure of the KNN thin films was determined by X-ray diffraction (XRD) measurements. Using an impedance meter, we compared the dielectric properties of the KNN thin films on unprocessed substrates with the dielectric properties of the KNN thin films on microcantilevers. Before piezoelectric measurements, we observed the initial deflection of each KNN microcantilever by a scanning electron microscope (SEM) and a laser interferometer.

The piezoelectric properties of the KNN films were evaluated from the actuator properties of the KNN/Si unimorph microcantilevers. The resonant frequencies of the KNN/Si microcantilevers were compared with their theoretical values. To evaluate the transverse piezoelectric properties, a negative unipolar sinusoidal voltage was applied between the top and bottom electrodes and the tip displacement of the unimorph cantilevers was measured by a laser Doppler vibrometer. For comparison, the piezoelectric property of the KNN thin films on unprocessed SOI substrates was also measured.

3. KNN films on Si microcantilevers

The XRD pattern of the KNN films is shown in Fig. 2. We could confirmed the growth of pyrochlore-free KNN films with polycrystalline perovskite phase on the SOI substrates having the Si microcantilevers. The KNN films were preferentially oriented along *c* axis in pseudocubic phase, and it is consistent with the previous study [8].

The SEM image of the KNN/Si unimorph cantilever with the length of 383 μm is shown in Fig. 3. The KNN/Si cantilevers were successfully fabricated without sticking to the substrate. On the other hand, the SEM observation revealed that a large initial deflection occurred for each KNN microcantilever. The initial tip deflection of each cantilevers were measured by the laser interferometer and the results were plotted in Fig. 4. According to the literature, the thermal expansion coefficient of KNN is larger than that of Si ($\alpha_{\mathrm{KNN}} = 8.0 \times 10^{-6}$ [1/°C], $\alpha_{\mathrm{Si}} = 2.6 \times 10^{-6}$ [1/°C]) [13, 14]. During the cooling process after KNN deposition from 680 to 25 °C, it appears that the KNN thin films suffered tensile stress from the Si layer, which caused the initial upward deflection of the KNN microcantilevers. The tip displacement y of the double-layered cantilever is given by the following equation,

$$y = -\frac{(\alpha_{KNN} - \alpha_{Si})L^2 \Delta T}{t_{KNN} + t_{Si} + \dfrac{4(E_{KNN} I_{KNN} + E_{Si} I_{Si})(t_{KNN} E_{KNN} + t_{Si} E_{Si})}{(t_{KNN} + t_{Si}) b t_{KNN} E_{KNN} t_{Si} E_{Si}}} \tag{1}$$

where α, ΔT, t, b, L, E, and I are thermal expansion coefficient, temperature change, thickness, cantilever width, cantilever length, Young's modulus, and second moment of area, respectively. The Young's moduli of <110>Si and KNN have been reported as 168 GPa and 104 GPa [15, 16]. We calculated initial deflection when the temperature of the substrate was cooled from 680 ˚C to 25 ˚C, and the calculation results of the deflection were also shown in Fig. 4. The calculated values were consistent with the measurements, thereby proving that the initial deflection was due to the mismatch of thermal expansion coefficients between the KNN thin films and the Si layer of the SOI substrate.

4. Piezoelectric properties of KNN microcantilevers

The frequency response of the tip displacement was measured by a laser Doppler vibrometer for the KNN/Si unimorph microcantilevers, and the results are plotted in Fig. 5. The resonant frequency of a KNN/Si double-layered cantilever is calculated from the following equation,

$$f = \frac{1}{2\pi}\left(\frac{1.875}{L}\right)^2 \sqrt{\frac{E_{KNN} I_{KNN} + E_{Si} I_{Si}}{\rho_{KNN} S_{KNN} + \rho_{Si} S_{Si}}} \quad (2)$$

where ρ and S are mass density and cross-section area, respectively. The densities of Si and KNN are reported 2331 kg/m^3 and 4250 kg/m^3, respectively [16, 17]. In calculation, we neglected the electrodes because of the thin thicknesses of them compared with those of the Si layer and the KNN thin film. As shown in Fig. 5, the resonant frequency of each microcantilever agrees well with the calculated results, indicating that the KNN microcantilevers were successfully fabricated with the designed length.

The relative dielectric constant of the KNN thin films on Si microcantilevers was 957–1072, and the dielectric loss (tanδ) was 0.038–0.058. On the other hand, the relative dielectric constant and tanδ of the KNN films on unprocessed thick Si substrates were 940–1029 and 0.039–0.048, respectively. These results imply that the direct deposition on Si microcantilevers does not influence the dielectric properties of the KNN films even though the thermal stress was partially released by the initial deflection of the cantilevers.

Figure 6 shows the tip displacements of the KNN microcantilevers as a function of the applied voltage. We applied negative unipolar sinusoidal voltage which was the same direction of polarization of KNN films. The frequency of the input voltage was 1 kHz which was considerably lower than the resonant frequency of the cantilevers. A large displacement of 7.6 μm could have been obtained for the 589-μm long cantilever at 20 V_{pp}. However, the tip displacement of each KNN microcantilever parabolically increased with the applied voltage.

Transverse piezoelectric coefficient d_{31} was calculated from the tip displacement δ of each fabricated KNN microcantilever as follows [18]:

$$\delta = -\frac{3 d_{31} V E_{Si} E_{KNN} t_{Si} (t_{Si} + t_{KNN}) L^2}{E_{KNN}^2 t_{KNN}^4 + 4 E_{Si} E_{KNN} t_{Si} t_{KNN}^3 + 6 E_{Si} E_{KNN} t_{Si}^2 t_{KNN}^2 + 4 E_{Si} E_{KNN} t_{Si}^3 t_{KNN} + E_{Si}^2 t_{Si}^4} \quad (3)$$

where V is the applied voltage. The transverse piezoelectric coefficient d_{31} of each KNN/Si microcantilever is plotted as a function of applied voltage in Fig. 7. From the tip displacement of each cantilever at 20 V_{pp}, the d_{31} of the KNN microcantilevers was calculated to be −53.5 pm/V. This result implies that the microactuators composed of the KNN thin films had piezoelectric properties compatible with those of the PZT thin films. However, because tip displacement parabolically increased with voltage, d_{31} of the KNN microcantilevers showed a large dependence on the applied voltage, i.e., d_{31}

almost proportionally increased with the applied voltage, as shown in Fig. 7. For comparison, we also measured the tip displacement of the unimorph cantilever composed of the KNN films on the unprocessed thick SOI substrates. A 537-μm thick (KNN: 2 μm, SOI: 535 μm), 1.79-mm wide, and 12.8-mm long unimorph cantilever was prepared and one end of the beam was cramped by a vise. The piezoelectric coefficient d_{31} was calculated according to Eq. (3) and the results are shown in Fig. 7. The piezoelectric coefficient d_{31} of the KNN films on the unprocessed thick SOI substrates were approximately 1.3 times larger than that of the KNN microcantilevers.

The transverse piezoelectric coefficient d_{31} of the KNN on both microfabricated and unprocessed SOI almost proportionally increased with the applied voltage. This implies that the generated strain increases with the square of the electric field, and it is similar to the electrostrictive effect. The large dependence on the applied voltage might be due to an extrinsic piezoelectric effect such as domain rotation [20]. In contrast, the electric field-induced strain under low external voltage was caused by the intrinsic piezoelectric effect. In Fig. 7, the extrapolation values of the d_{31} at zero electric field are approximately -5×10^{-12} and -20×10^{-12} m/V for the KNN microcantilevers and the KNN/SOI, respectively. This result suggests that the intrinsic d_{31} of the KNN microcantilevers is lower than that of KNN on the unprocessed thick substrate; the reason for which is presently unclear. However, the release of the internal stress by initial bending of the cantilever might influence the piezoelectric motion of the KNN films. On the other hand, compared with the intrinsic d_{31} at zero electric field, the tendency of the increasing of d_{31} is almost the same for both unimorphs. It indicates that the extrinsic piezoelectric effect is almost independent of the microfabrication process of the KNN films.

The tip displacement under the bipolar sinusoidal voltage was measured at 700-Hz frequency and the displacement loops are plotted in Fig. 8. The KNN unimorph actuators of both the Si microcantilevers and the unprocessed SOI show typical butterfly loops originating from the domain rotation of the ferroelectric materials. However, the coercive electric field of the KNN microcantilever was larger and the curves at the coercive electric field, in which domain switching occurs, were rounded than that of the KNN films on unprocessed substrates. In the case of KNN microcantilevers, the microcantilevers were initially deflected upward as shown in Fig. 3, and considering that the downward displacement was as small as 0.1 μm in Fig. 8, the difference of the hysteresis loops was not caused by the touch of the tip of the KNN microcantilevers to the substrates. Upward initial deflection caused the partial release of tensile residual stress of the KNN films, and it would be attributed to the difference of the piezoelectric

characteristics of the KNN microcantilevers from the KNN films on the unprocessed substrates.

In this study, we successfully fabricated lead-free piezoelectric KNN microcantilevers by direct deposition on microfabricated SOI substrates. This method is very useful for developing microdevices composed of functional thin films, which is difficult for a conventional etching process. Furthermore, we revealed that the characteristic behavior of the microfabricated KNN thin films in the shape of microcantilevers differs from the piezoelectric properties of the KNN films on thick Si substrates.

5. Conclusions

We fabricated micro-cantilevers of lead-free KNN thin films on the Si substrate and evaluated their transverse piezoelectric properties. After releasing Si micro-cantilevers from the SOI substrates, KNN thin films with perovskite structure were directly deposited by RF-sputtering. This method enables to fabricate lead-free KNN unimorph micro-cantilevers without microfabrication of the KNN thin films using conventional etching process. The application of 20 V_{pp} between top and bottom electrodes generated the tip displacement of 7.6 μm for the 589 μm-long micro-cantilever and the transverse piezoelectric coefficient d_{31} of each micro-cantilevers was calculated to be -53.5 pm/V at 20 V_{pp}, although d_{31} strongly depends on the applied voltage. The tip displacement increased parabolically with the applied voltage due to extrinsic piezoelectric effect. The intrinsic piezoelectric effect of the KNN unimorph micro-actuator was smaller than that of the KNN on the unprocessed substrates, while the extrinsic piezoelectric effect was almost same between the KNN micro-cantilevers and the KNN on unprocessed SOI substrates.

References

[1] S. Trolier-McKinstry and P. Muralt, Thin film piezoelectrics for MEMS, J. Electroceram. 12 (2004) 7-17.

[2] Y. Saito, H. Takao, T. Tani, T. Nonoyama, K. Takatori, T. Homma, T. Nagaya, and M. Nakamura, Lead-free piezoceramics, Nature 432 (2004) 84-87.

[3] T. R. Shrout and S. J. Zhang, Lead-free piezoelectric ceramics: Alternatives for PZT? J. Electroceram. 19 (2007) 111-124.

[4] M. Blomqvist, J-H. Koh, S. Khartsev, A. Grishina, and J. Andreasson, High-performance epitaxial $Na_{0.5}K_{0.5}NbO_3$ thin films by magnetron sputtering, Appl. Phys. Lett. 81 (2002) 337-339.

[5] H. J. Lee, I. W. Kim, J. S. Kim, C. W. Ahn, and B. H. Park, Ferroelectric and piezoelectric properties of $Na_{0.52}K_{0.48}NbO_3$ thin films prepared by radio frequency magnetron sputtering, Appl. Phys. Lett. 94 (2009) 092902.

[6] T. Saito, T. Wada, H. Adachi, and I. Kanno, Pulsed laser deposition of high-quality $(K,Na)NbO_3$ thin films on $SrTiO_3$ substrate using high-density ceramic targets, Jpn. J. Appl. Phys. 43 (2004) 6627-6631.

[7] I. Kanno, T. Mino, S. Kuwajima, T. Suzuki, H. Kotera, and K. Wasa, Piezoelectric properties of $(K,Na)NbO_3$ thin films deposited on $(001)SrRuO_3/Pt/MgO$ substrates, IEEE Trans. Ultrason. Ferroelectr. Freq. Control. 54 (2007) 2562-2566.

[8] K. Shibata, F. Oka, A. Ohishi, T. Mishima, and I. Kanno, Piezoelectric properties of $(K,Na)NbO_3$ films deposited by RF magnetron sputtering, Appl. Phys. Express 1, (2008) 011511.

[9] K. Zheng, J. Lu, and J. Chu, A novel wet etching process of $Pb(Zr,Ti)O_3$ thin films for applications in microelectromechanical system, Jpn. J. Appl. Phys. 43 (2004) 3934-3937.

[10] J-K. Jung and W-J. Lee, Dry etching characteristics of $Pb(Zr,Ti)O_3$ films in CF_4 and Cl_2/CF_4 inductively coupled plasmas, Jpn. J. Appl. Phys. 40 (2001) 1408-1419.

[11] C. M. Kang, G-H. Kim, K-T. Kim, and C-I Kim, Etching characteristics of $(Na_{0.5}K_{0.5})NbO_3$ thin films in an inductively coupled Cl_2/Ar plasma, Ferroelectrics 357 (2007) 179-184.

[12] Y. Xu, D. Liu, F. Lai, Y. Zhen, and J-F. Li, Fabrication of $(K,Na)NbO_3$ Lead-Free Piezoceramic microrod arrays by Sol–Gel processing with micromachined silicon templates, J. Am. Ceram. Soc. 91 (2008) 2844-2847.

[13] K. Shibata, K. Suenaga, A. Nomoto, and T. Mishima, Curie temperature, biaxial elastic modulus, and thermal expansion coefficient of $(K,Na)NbO_3$ piezoelectric

thin films, Jpn. J. Appl. Phys. 48 (2009) 121408.
[14] M. M. de Lima, Jr., R. G. Lacerda, J. Vilcarromero, and F. C. Marques, Coefficient of thermal expansion and elastic modulus of thin films, J. Appl. Phys. 86 (1999) 4936-4942.
[15] J. C. Greenwood, Silicon in mechanical sensors, J. Phys. E: Sci. Instrum. 21 (1988) 1114-1128.
[16] L. Egerton and D. M. Dillon, Piezoelectric and dielectric properties of ceramics in the system potassium—sodium niobate, J. Am. Ceram. Soc. 42 (1959) 438-442.
[17] H. J. McSkimin, W. L. Bomd, E. Buehler, and G. K. Teal, Measurement of the elastic constants of silicon single crystals and their thermal coefficients, Phys. Rev. 83 (1951) 1080
[18] J. G. Smits and W-S. Choi, The constituent equations of piezoelectric heterogeneous bimorphs, IEEE Trans. Ultrason. Ferroelectr. Freq. Control, 38 (1991) 256-270.
[19] I. Kanno, H. Kotera, and K. Wasa, Measurement of transverse piezoelectric properties of PZT thin films, Sens. Actuators A 107 (2003) 68-74.
[20] F. Xu, S. Trolier-McKinstry, W. Ren, B. Xu, Z.-L. Xie, and K. J. Hemker, Domain wall motion and its contribution to the dielectric and piezoelectric properties of lead zirconate titanate films, J. Appl. Phys. 89 (2001) 1336-1348.

Fig. 1 Fabrication process of KNN/Si unimorph microcantilevers; (a) SOI substrate with the Si and SiO_2 layers of 8μm and 2μm, respectively. (b) Si layer is fabricated into cantilever structures by dry etching. (c) SiO_2 under the cantilevers is etched by buffered HF. (d) Pt/Ti layers are deposited by RF-sputtering. (e) KNN piezoelectric films are deposited by RF-sputtering. (f) Pt top electrodes are deposited on the KNN films and patterned by a lift-off process.

Fig. 2 XRD patterns of KNN thin films on SOI substrate having microcantilevers. Pyrochlore-free KNN films with a preferential *c*-axis orientation were grown on Pt/Ti-coated SOI substrates on which microcantilevers were fabricated.

Fig. 3 SEM image of KNN/Si unimorph microcantilever. KNN/Si microcantilever is released from the substrate.

Fig. 4 Initial deflection of KNN/Si microcantilevers as a function of the cantilever length. Filled circles and solid line represent the experimental values and calculation result, respectively.

Fig. 5 Resonant frequency of the KNN/Si microcantilevers as a function of the cantilever length. Filled circles and solid line represent the experimental values and calculation result, respectively.

Fig. 6 Tip displacement of KNN/Si microcantilevers as a function of applied voltage. The tip displacement of each KNN microcantilever parabolically increased with the applied voltage.

Fig. 7 Transverse piezoelectric coefficient d_{31} of KNN films on Si microcantilevers as a function of applied voltage. The cross marks represent d_{31} of KNN films on unprocessed SOI substrates.

Fig. 8 Hysteresis loops of tip displacement vs. bipolar electric field for KNN unimorphs on microcantilever and unprocessed SOI cantilever.

1. SOI Substrate

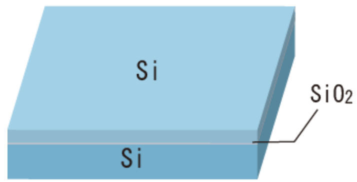

2. Si Dry Etching

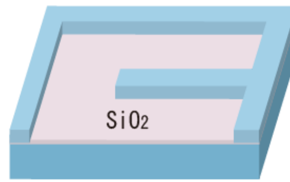

3. SiO2 Wet Etching

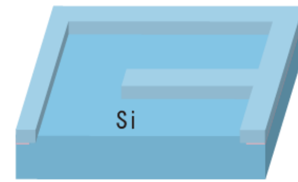

4. Ti/Pt Sputtering

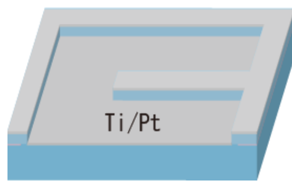

5. KNN Sputtering

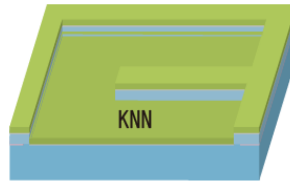

6. Pt Patterning

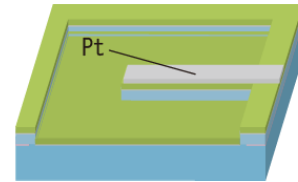

Fig.1

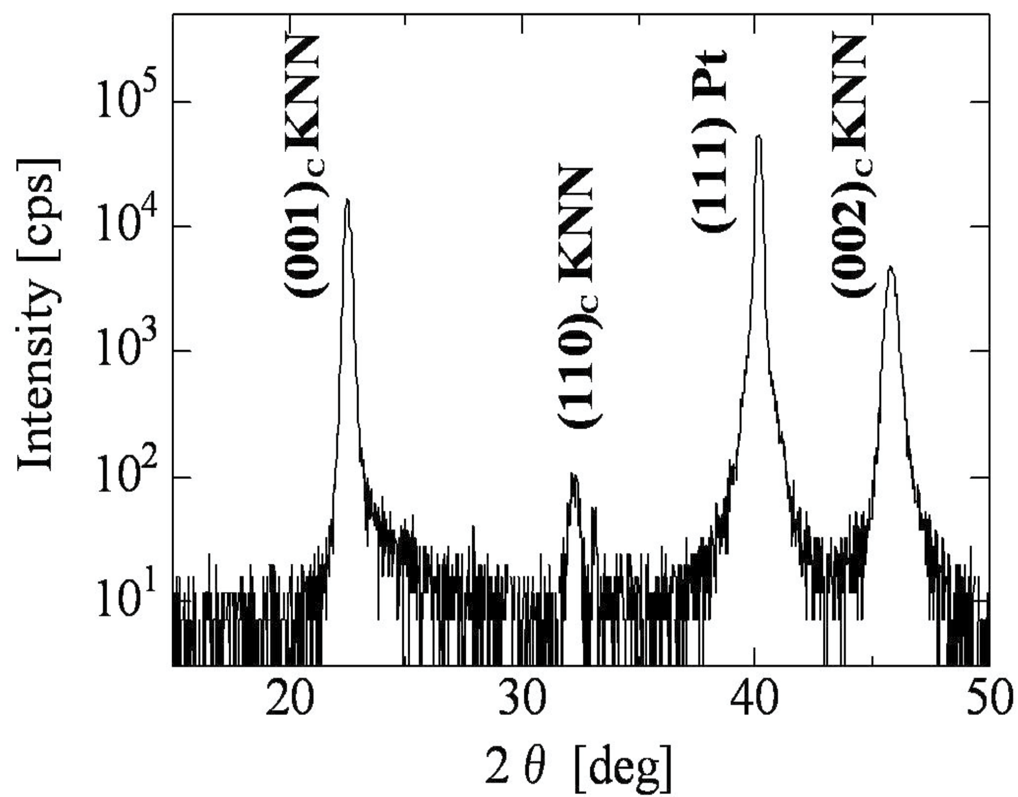

Fig.2

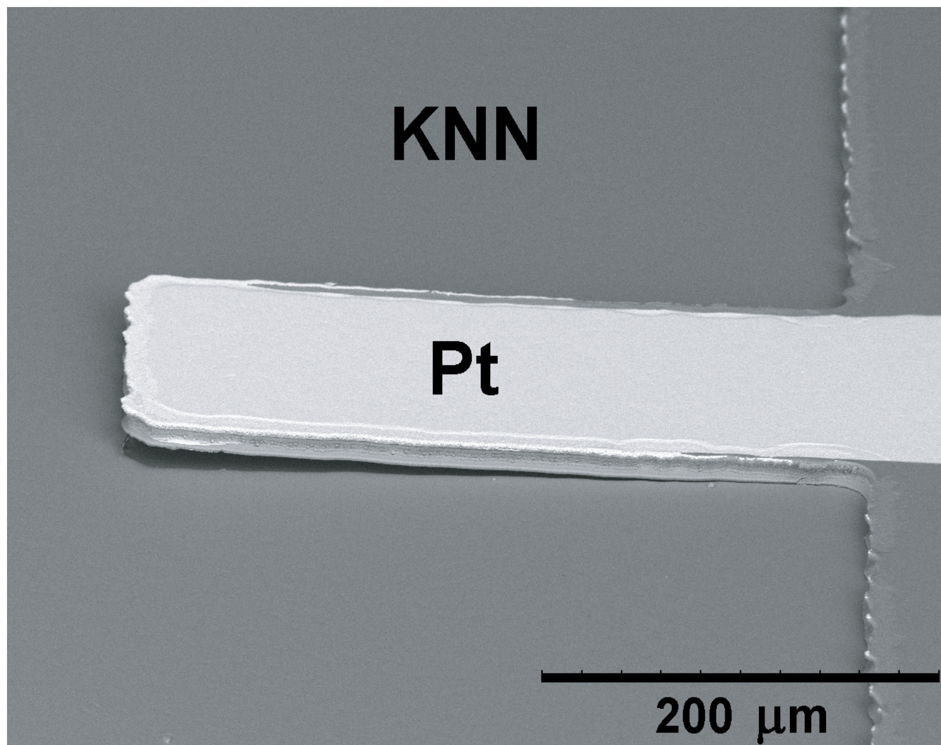

Fig.3

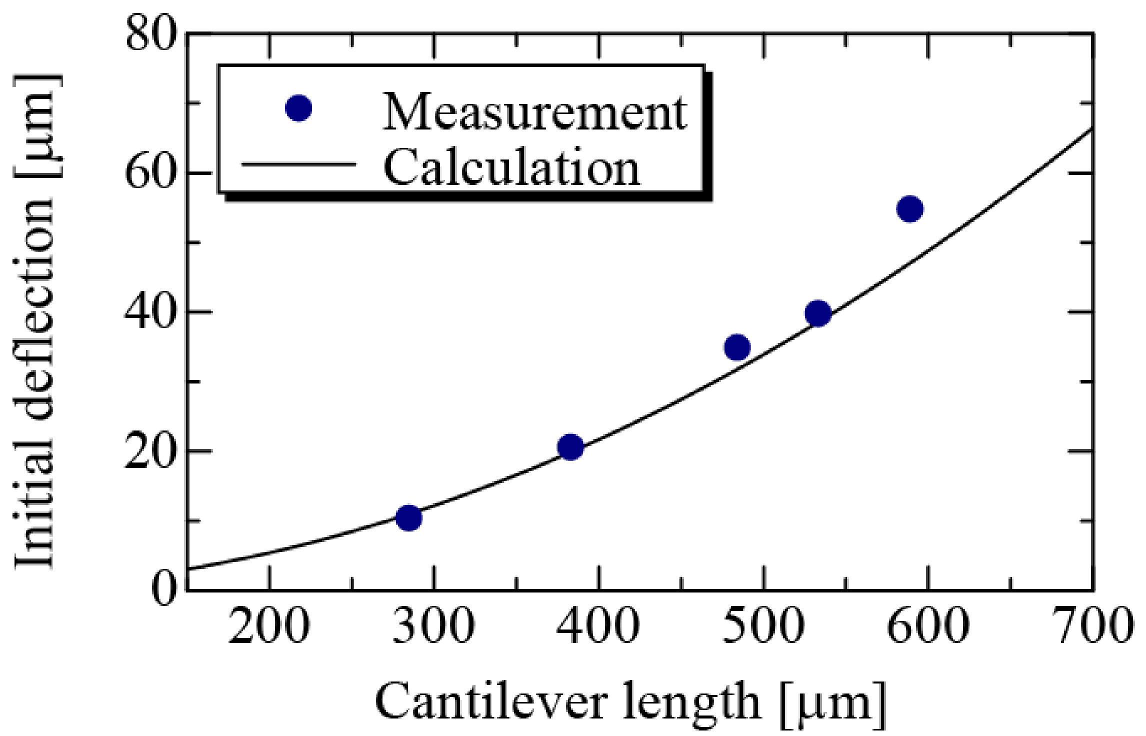

Fig. 4

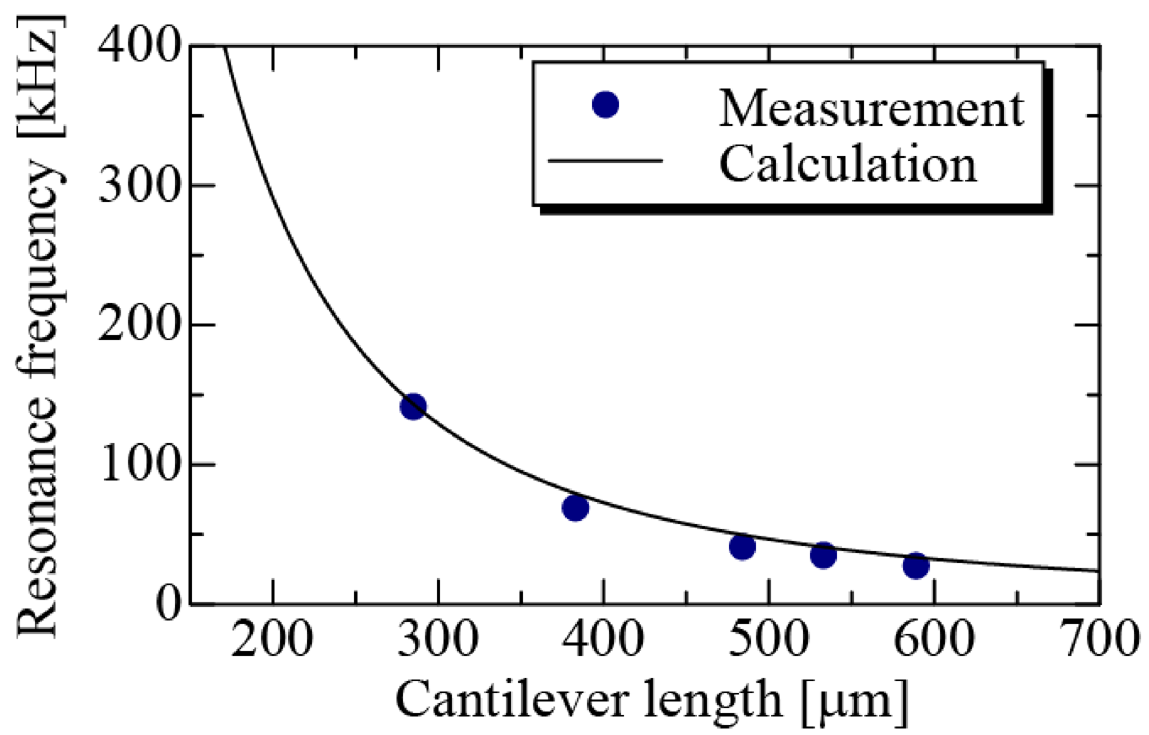

Fig. 5

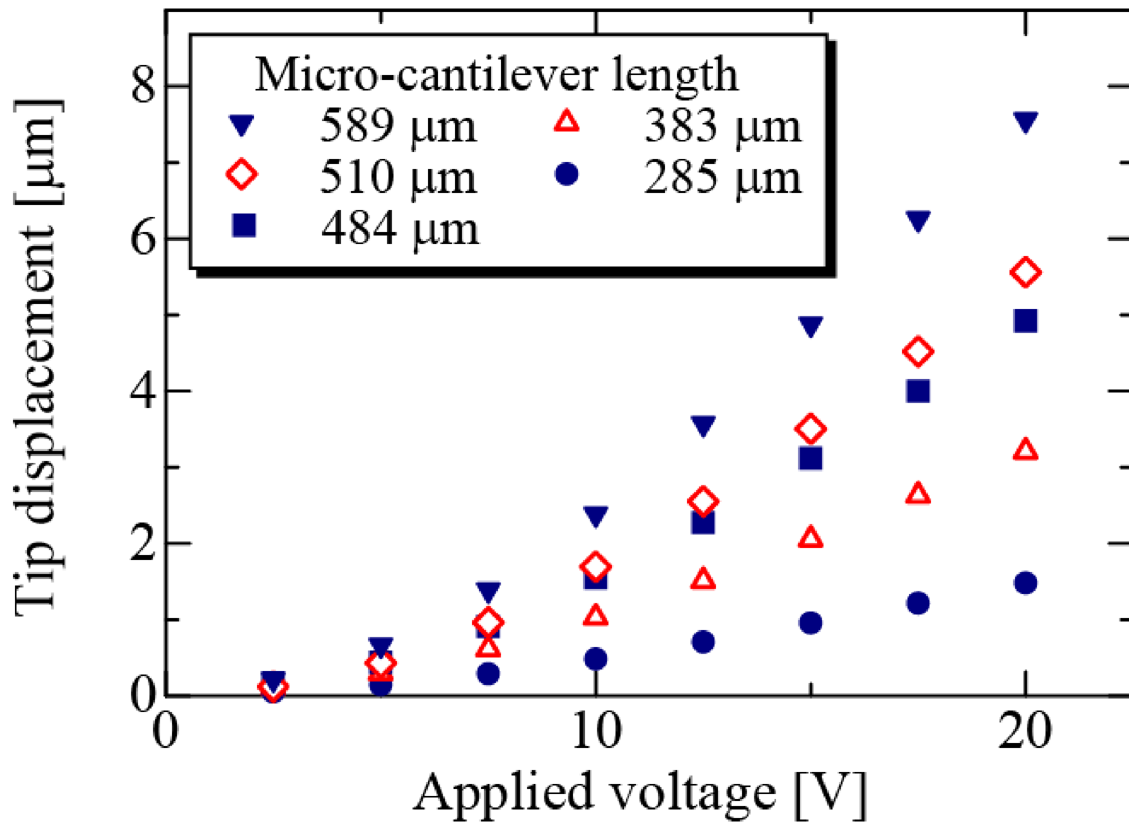

Fig. 6

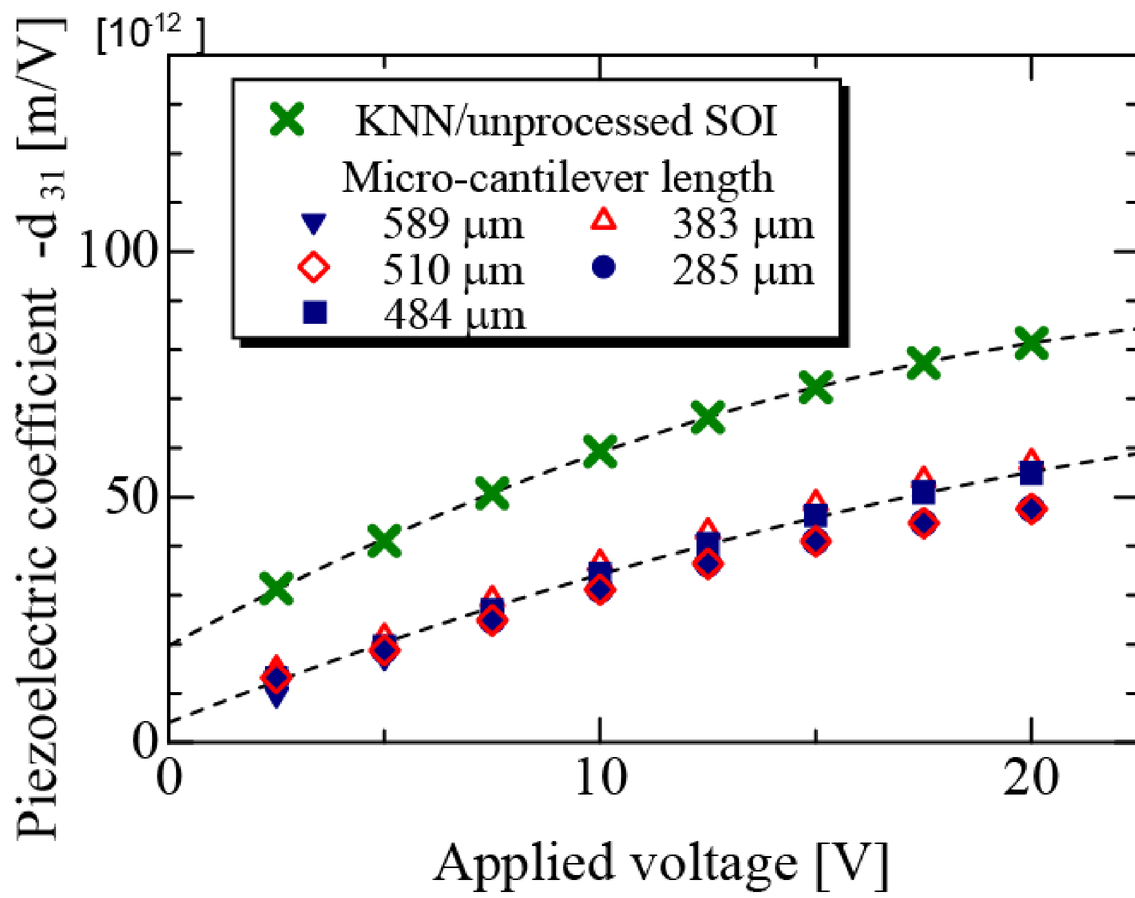

Fig. 7

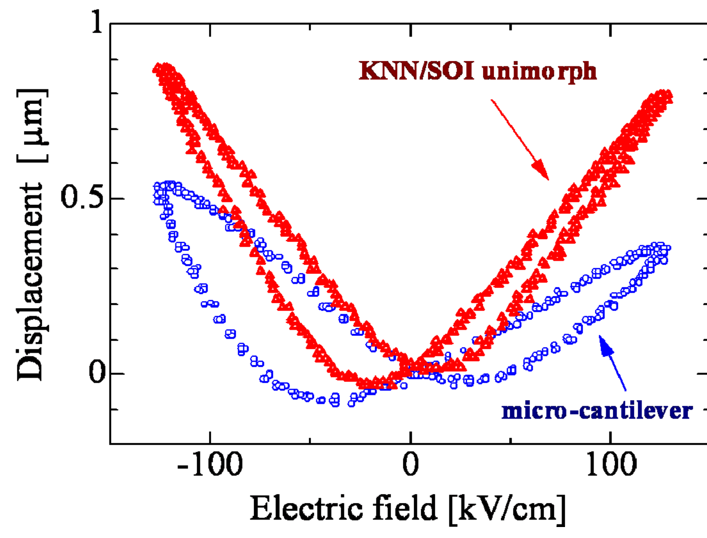

Fig. 8